Modulation of the Extracellular Matrix in Advanced Atherosclerosis

Nooijer, Ramon de

7 Leukocyte Cathepsin K Influences Atherosclerotic Lesion Composition and Bone Mineral Density in LDL-Receptor Deficient Mice

J. Guo[1], M. van Eck[1], R. de Nooijer[1,2], H.J. de Bont[3], S.J. Hoffman[4], G.B. Stroup[4], E.A.L. Biessen[1], G.M. Benson[5], P.H.E. Groot[5], Th.J.C. van Berkel[1]

[1] Div. of Biopharmaceutics, Leiden University, Leiden, Netherlands;
[2] Dept. of Cardiology, Leiden University Medical Center, Leiden, Netherlands;
[3] Division of Toxicology, Leiden University, Leiden, Netherlands;
[4] Department of Bone and Cartilage Biology, GlaxoSmithKline Pharmaceuticals, King of Prussia, PA 19406, USA;
[5] Atherosclerosis Department, GlaxoSmithKline Pharmaceuticals, Stevenage, UK.

Submitted

Abstract

Cathepsin K (Cat K), an established drug target for osteoporosis, has recently been reported to be present in atherosclerotic lesions. Due to its proteolytic activity Cat K may influence the atherosclerotic lesion composition and stability. To assess the biological role of leukocyte Cat K, we used the technique of bone marrow transplantation to selectively disrupt Cat K in the hematopoietic system. Total bone marrow progenitor cells from Cat $K^{+/+}$, Cat $K^{+/-}$ and Cat $K^{-/-}$ mice were transplanted into X-ray irradiated LDL receptor knockout ($LDLR^{-/-}$) mice. The selective silencing of leukocyte Cat K resulted in phenotypic changes in bone formation with an increased total bone mineral density in the Cat $K^{-/-} \rightarrow LDLR^{-/-}$ mice and an effect of gene dosage. In relation to atherogenesis, absence of leukocyte Cat K resulted in dramatically decreased collagen and modestly increased macrophage content of the atherosclerotic lesions but no difference as to lesion size was observed. Further characterization of the atherosclerotic lesions revealed less elastic lamina fragmentation and a significant increase of apoptotic and necrotic area in Cat $K^{-/-} \rightarrow LDLR^{-/-}$ mice. *In vitro* Cat K inhibition in oxLDL treated THP-1 cells also led to a significantly increased cell death via both apoptosis and necrosis, consistent with the increase of both apoptotic and necrotic area observed in the Cat $K^{-/-} \rightarrow LDLR^{-/-}$ mice.
In conclusion, leukocyte Cat K is important for atherosclerotic plaque composition, vulnerability and bone remodeling, making it an attractive target for pharmaceutical modulation in atherosclerosis and osteoporosis.

Introduction

Remodeling of the extracellular matrix of blood vessels as well as bone resorption vs. formation is a life-long continuously changing and dynamic process. Imbalance of this process could lead to the clinical manifestation of e.g. osteopetrosis/osteoporosis or the phenotypic changes in atherosclerotic lesion development. Several research groups have cloned the cysteine protease cathepsin K (Cat K), from mouse, rabbit and human cDNA libraries[1-4]. Studies of the role of Cat K have focused primarily on its function in bone remodeling. Cat K, which is highly expressed in osteoclasts[5], has been shown to degrade bone collagen as well as other bone matrix proteins[6;7]. Mutations in the Cat K gene have been identified as the underlying cause of the relatively rare human osteopetrotic disease, pycnodysostosis[8;9]. Targeted mutation of the Cat K gene in mice results in many of the phenotypic features of pycnodysostosis, including increased bone mineral density and bone deformation[10;11]. Administration of Cat K antagonists in mice successfully inhibited bone resorption both *in vitro* and *in vivo*[12]. Recently, Sukhova *et al*[13] found that Cat K is overexpressed in human atheroma, raising the possibility of its functional role outside the bone, for instance, in extracellular matrix remodeling of atherosclerotic lesions. This might have important consequences for plaque stability and its susceptibility to rupture. However, no direct evidence about the function of Cat K in atherosclerosis has yet been described.
Bone marrow transplantation (BMT) is a useful technique to specifically study the leukocyte specific role of genes involved in atherogenesis[14;15]. To investigate the potential role of leukocyte Cat K in atherosclerotic remodeling of the arterial wall, we irradiated low-density lipoprotein receptor knockout mice ($LDLR^{-/-}$), a well-documented model for atherosclerosis[16;17], and reconstituted the hematopoietic systems with the total bone marrow progenitor cells from Cat K wild-type ($Cat\ K^{+/+}$), heterozygous ($Cat\ K^{+/-}$) and knockout ($Cat\ K^{-/-}$) mice. In these studies we also monitored the effect of this bone marrow progenitor cell replacement on bone remodeling. It appears that Cat K originated from bone marrow progenitor cells not only influences the bone mineral density, but also importantly affects cellular and matriceal composition of the atherosclerotic plaque.

Materials and Methods

Animals

Cat $K^{+/+}$, Cat $K^{+/-}$, and Cat $K^{-/-}$ mice were used as donors for BMT and generated as previously described[10]. $LDLR^{-/-}$ recipient mice were obtained from the Jackson Laboratory as mating pairs and bred at the Gorlaeus Laboratories, Leiden, The Netherlands. Mice were housed in sterilized filter-top cages and fed a sterilized regular chow diet, containing 5.7% w/w fat (Hope Farms, Woerden, The Netherlands). Four weeks after BMT, the diet was switched to a high-fat diet containing 0.25% w/w cholesterol (Special Diet Services, Whitham, Essex, UK) for another 12 weeks in order to induce atherosclerosis. Drinking water was supplied with antibiotics (83 mg/L ciprofloxacin and 67 mg/L polymyxin B sulfate) and 6.5g/L sugar.

Bone Marrow Transplantation and Chimerism Analysis of Recipient Mice after BMT

To induce bone marrow aplasia, female $LDLR^{-/-}$ mice (n=37), 7 weeks of age, were exposed to a single dose of 9 Gy (0.28 Gy/min, 200kV, 4mA) X-ray total body irradiation as described.[15;18] The following day, mice received 0.5×10^7 bone marrow progenitor cells isolated from Cat $K^{+/+}$, Cat $K^{+/-}$, and Cat $K^{-/-}$ mice (age 8 weeks), through tail vein injection. The hematopoietic chimerism of the $LDLR^{-/-}$ mice was determined by genomic DNA genotyping from peripheral blood leukocytes, at 16 weeks after BMT. Cat K forward: 5'-ATGGTCTCTCTAAACCTTTGG-3' and Cat K reverse: 5'-ACCTGGTTCTTGACTGGAGTAACG-3' primers were used during PCR using the following programs: 94°C for 5 min; 94°C for 30 sec, 55°C for 30 sec, 72°C for 1.5 min, for 30 cycles; 72 °C for 10 min. Semiquantitative PCR was set up by mixing the genomic DNA

from both wild-type and knockout animals, ranging from 0%, 10%, 20%, 30%, 40%, 50%, 60%, 70%, 80%, 90%, 95%, 98%, 99% and up to 100% of knockout vs. wild-type. Final PCR products were separated on 1% agarose gel.

Serum Cholesterol and Triglycerides Analysis

After an overnight fasting period, approximately 100 µL blood was drawn from each individual mouse by tail bleeding. The concentrations of total cholesterol and triglycerides in the serum were determined using enzymatic procedures (Roche, Germany), according to the manufacturer's instructions. Precipath (standardized serum; Roche, Germany) was used as internal standard.

Histological Analysis of Aortic Roots

To analyze the atherosclerotic lesions, $LDLR^{-/-}$ mice were sacrificed at 16 weeks after BMT (4 weeks on regular chow diet followed by 12 weeks on Western-type diet). The arterial tree was perfusion-fixed (Zinc Formal Fixx, Shandon, UK) and atherosclerosis was analyzed as described[19]. Mean lesion area (in μm^2) was calculated from 10 oil red O stained sections from each mouse, starting at the appearance of the tricuspid valves. The macrophage infiltration in the atherosclerotic lesions was determined after 12 weeks Western-type diet feeding by immunohistochemistry using rabbit-anti-mouse CD68 antibody (kindly provided by S. Gordon, Sir William Dunn School of Pathology, University of Oxford, UK; 1:500 dilution). The collagen content of the lesions was visualized with aniline blue by Masson's Trichrome staining according to the manufacturer's instructions (Sigma Diagnostics). The CD68 positive and collagen content of lesions were subsequently calculated as the percentage of positive area vs. mean lesion area (5 sections from each mouse).The mean necrotic core area, was carefully examined as described by Virmani *et al* previously[20], and calculated as the percentage of mean necrotic area vs. mean lesion area (5 sections from each mouse). For detection of DNA fragmentation, terminal deoxynucleotide transferase-mediated dUTP nick end labeling (TUNEL) staining for apoptosis in atherosclerotic lesions was performed using the In Situ Cell Death Detection Kit (Roche) as previously described by Gavrieli *et al*[21]. TUNEL-positive nuclei were visualized by Nova Red (Vector) and sections were counterstained with 0.3% methylgreen. Sections treated with DNase (2U/section) served as a positive control. Cell death was expressed as percentage TUNEL positive nuclei to total nuclei in the neointima. All quantifications were done blind in 13 mice for Cat $K^{+/+}\rightarrow$ $LDLR^{-/-}$, 11 mice for Cat $K^{+/-}\rightarrow$ $LDLR^{-/-}$ and 13 mice for Cat $K^{-/-}\rightarrow$ $LDLR^{-/-}$ group, by computer-aided morphometric analysis using the Leica image analysis system.

Preservation of Elastic Lamina of Aortic Roots

To analyze the effect of Cat K deficiency on the preservation of the elastic lamina, oil red O-stained sections of the aortic root were examined under a fluorescence microscope for the discontinuities of elastic lamina, which exhibits auto-fluorescence under a 465-495 nm excitation filter and a 515-555 nm emission filter. The number of breakdowns of elastic lamina of each mouse were added up together within each group and calculated as the frequency of fragmentation (= average number of lamina ruptures/mouse).

Potential Involvement of Cat K in Macrophage Cell Death

Human monocytic THP-1 cells were cultured in RPMI 1640 medium supplemented with 10% fetal calf serum, 2 mM L-glutamine, 100 µg/mL streptomycin and 100 U/mL penicillin. Native low-density lipoprotein (LDL) was purified by ultracentrifugation from healthy human blood and subsequently oxidized at the presence of 10 µM of $CuSO_4$ as described[22]. Oxidization was confirmed by the change in electrophoretic mobility on agarose gel electrophoresis at 60 mA for 6 hours. THP-1 cells were first incubated for 30 minutes with 1 µM of Cat K inhibitor[23]{1-(N-Benzyloxycarbonyl-leucyl)-5-(N-Boc-phenylalayl-leucyl)carbohydrazide Inhibitor Boc-I, Calbiochem}, and then treated with 100 µg/mL of oxLDL for 24 hours to induce cell death[24]. Cells were subsequently stained with Magic Red Cathepsin Kit (Immunochemistry Technologies, LLC) according to the manufacturer's instructions, and placed under fluorescence microscope to visualize Cat K activity, using a 510-560 nm excitation filter and a 570-620 nm emission filter. To address the potential role Cat K in oxLDL-induced cell death of monocytes/macrophage, THP-1 cells were first subjected to the same conditions for the induction of cell death as indicated above, either treated with or without 1 µM of Cat K inhibitor, and then incubated for 15 minutes with Annexin V and propidium iodide allowing the discrimination of apoptotic and necrotic cells by FACS analysis.

Peripheral Quantitative Computed Tomographic Analysis of Tibias

To investigate the role of leukocyte Cat K in bone remodeling, right proximal tibias of the transplanted mice were evaluated by peripheral Quantitative Computer Tomography (pQCT) using the Stratec/Norland Research M (Norland Medical Systems, Inc., Fort Atkinson, WI). Quality control of the instrument was carried out each day prior to and after sample analysis by scanning a cone phantom of known density. A cone scan was performed in the AM and a standard scan was performed following sample analysis. Scans were made *ex vivo* on the right proximal tibia. A 3-D 0.5 mm slice was taken at a point 15% of the length between the tibia-fibula junctions distal to the most proximal tibia-fibula junction. Settings for the mask were as follows: object length, 100 mm; voxel size, 0.07 mm; diameter, 10 mm; speed, 2 mm/sec; number of blocks, 1; scout view (SV) speed, 20 mm/sec; and SV distance between lines, 0.5 mm. BMD, bone mineral content (BMC), and bone area was determined for the total, trabecular, subcortical & cortical, and cortical

regions. Analysis was as follows: Calcbd was set at contour mode 2, peel mode 2, inner threshold 400 mg/cm^3 and Cortbd was separation mode 2 and threshold 400 mg/cm^3. 13 mice were analyzed for Cat $K^{+/+}$→ $LDLR^{-/-}$, 11 mice for Cat $K^{+/-}$→ $LDLR^{-/-}$, and 13 mice for Cat $K^{-/-}$→ $LDLR^{-/-}$ group.

Statistical Analysis
All values are displayed as mean±SEM. Differences in plaque morphometry were statistically analyzed for significance using the Mann-Whitney U test. Collagen, elastic lamina ruptures, TUNEL positivity, SMC and macrophage content were compared using the 2-tailed Student's *t*-test.

Results

Generation of $LDLR^{-/-}$ Mice with Specific Deficiency in Leukocyte Cat K

To assess the biological role of leukocyte Cat K both in arterial and bone remodeling, we a bone marrow transplantation to selectively disrupt Cat K in the hematopoietic system. Bone marrow progenitor cells from Cat $K^{+/+}$, Cat $K^{+/-}$, and Cat $K^{-/-}$ mice were transplanted into irradiated $LDLR^{-/-}$ mice. Reconstitution of the hematopoietic system in recipients of Cat $K^{+/+}$, Cat $K^{+/-}$ and Cat $K^{-/-}$ marrow was demonstrated by PCR of genomic DNA from peripheral blood leukocytes at 16 weeks after BMT (Fig 1A). PCR amplification of the wild-type allele produces a 518 bp product in recipients transplanted with Cat $K^{+/+}$ and Cat $K^{+/-}$ marrow, and amplification of the mutant allele produces a 1.7 kb product in transplanted with Cat $K^{+/-}$ and Cat $K^{-/-}$ marrow. We also detected a faint wild-type PCR product in recipients of Cat $K^{-/-}$ marrow. However, semiquantitative PCR analysis demonstrated that more than 98% of the peripheral blood leukocytes were of Cat $K^{-/-}$ donor origin (Fig 1B).

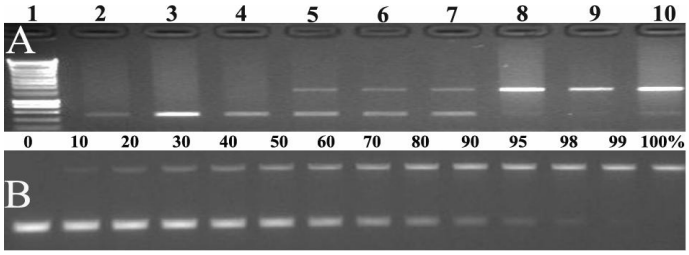

Figure 1. Generation of $LDLR^{-/-}$ mice with specific deficiency in leukocyte Cat K. Genomic DNA from peripheral blood leukocytes was extracted and used for PCR amplification **(A)** lane 1, DNA marker; lane 2-4, Cat $K^{+/+}$→ $LDLR^{-/-}$ mice, which displayed 518 bp wild-type bands; lane 5-7, Cat $K^{+/-}$→ $LDLR^{-/-}$ mice, which displayed both 518 bp wild-type bands and 1.7 kb knockout bands; lane 8-10, Cat $K^{-/-}$→ $LDLR^{-/-}$ mice, which displayed prominent 1.7 kb knockout bands with only faint 518 bp wild-type bands. **(B)** Semiquantitative PCR by mixing the genomic DNA from both wild-type and knockout animals, ranging from 0%, 10%, 20%, 30%, 40%, 50%, 60%, 70%, 80%, 90%, 95%, 98%, 99% and up to 100% of knockout vs. wild-type, demonstrates that more than 98% of the peripheral blood leukocytes are of Cat $K^{-/-}$ origin.

Effect of Leukocyte Cat K Deficiency on Serum Total Cholesterol and Triglyceride Levels

During the weeks following BMT, total plasma cholesterol levels were closely monitored. No differences between Cat $K^{+/+}$→ $LDLR^{-/-}$, Cat $K^{+/-}$→ $LDLR^{-/-}$, and Cat $K^{-/-}$→ $LDLR^{-/-}$ mice could be observed at 4 weeks after BMT and plasma cholesterol was not significantly different from baseline levels. In order to induce atherosclerotic lesion formation, the transplanted $LDLR^{-/-}$ mice were fed a high-fat diet, starting at week 4 after BMT. As a result, total plasma cholesterol in both control and experimental groups increased approximately 2-fold at week 8 and 4-fold at week 12 and 16, respectively (Fig 2A) but still no differences could be detected between groups. Although variations in plasma triglyceride levels (Fig 2B) could be observed between groups before and at different time points after BMT, none of these reached statistical significance.

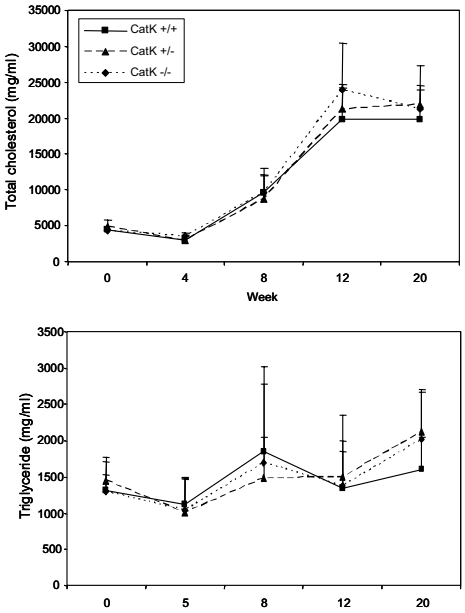

Figure 2. Effect of leukocyte Cat K deficiency on serum total cholesterol and triglycerides levels. Blood samples were drawn after an overnight fast at the indicated time points and serum cholesterol and triglyceride levels were analyzed. Absence of leukocyte Cat K does not significantly influence the total cholesterol and triglyceride levels. Values represent the mean ± SEM.

Effect of Leukocyte Cat K Deficiency on Bone Remodeling

Peripheral quantitative computed tomography analysis of the proximal tibias revealed a Cat K dose-dependent effect on bone mineral density. Significantly increased total bone mineral density in Cat $K^{-/-}$→ $LDLR^{-/-}$ mice to 793±11.5 mg/cm^3 could be observed, compared to 735.9±16.6 mg/cm^3 and 757.5±12.6 cm/cm^3 in Cat $K^{+/+}$→ $LDLR^{-/-}$ and Cat $K^{+/-}$→ $LDLR^{-/-}$ mice, respectively ($P< 0.05$). The increase in total BMD was a direct result of a larger amount of cortical bone, probably due to impaired osteoclastic bone resorption in the absence of Cat K. There was very little trabecular bone mass observed in any of the groups. Moreover, a tendency to a decreased tibia length was observed in absence of Cat K (Fig 3).

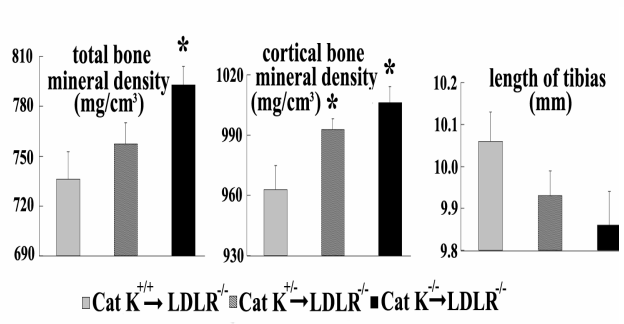

Figure 3. Effect of leukocyte Cat K deficiency on bone morphology. Disruption of leukocyte Cat K results in a gene dosage effect on total bone mineral density, cortical bone mineral density and length of tibias. Values represent the mean ± SEM. Statistically significant difference of $P<0.05$, compared with Cat $K^{+/+}\rightarrow LDLR^{-/-}$ mice.

Effect of Leukocyte Cat K on Atherosclerotic Lesion Development

To determine the effects of leukocyte Cat K deficiency on the formation of atherosclerotic lesions, the hearts and aortas of the $LDLR^{-/-}$ mice, transplanted with either Cat $K^{+/+}$, Cat $K^{+/-}$, or Cat $K^{-/-}$ bone marrow progenitor cells, were perfused and fixed at 16 weeks after BMT. Representative photomicrographs of the aortic roots of Cat $K^{+/+}\rightarrow LDLR^{-/-}$, Cat $K^{+/-}\rightarrow LDLR^{-/-}$, and Cat $K^{-/-}\rightarrow LDLR^{-/-}$ mice are shown in Fig 4A. Mean lesion area did not differ between groups (Cat $K^{+/+}\rightarrow LDLR^{-/-}$: $5.9\pm2.8\times10^5$ μm^2; Cat $K^{+/-}\rightarrow LDLR^{-/-}$: $5.9\pm1.7\times10^5$ μm^2; Cat $K^{-/-}\rightarrow LDLR^{-/-}$ $6.2\pm1.1\times10^5$ μm^2). Quantitative morphological analysis of the atherosclerotic plaques revealed that 31.3±9.8% and 35.3±10.2% of the lesions consisted of infiltrated macrophages in Cat $K^{+/+}\rightarrow LDLR^{-/-}$ and Cat $K^{+/-}\rightarrow LDLR^{-/-}$ mice, respectively, while intimal macrophage content increased to 53.1±8.1% with leukocyte CatK deficiency ($P<0.05$, Fig 4B). Conversely, collagen content decreased dramatically to 8.6±3.3% ($P<0.001$) in Cat $K^{-/-}\rightarrow LDLR^{-/-}$ mice compared to 49.6±11.5% in Cat $K^{+/+}\rightarrow LDLR^{-/-}$ and 42.8±12.6% in Cat $K^{+/-}\rightarrow LDLR^{-/-}$ mice (Fig 4C). The percentage of mean necrotic area vs. mean lesion area was 5.6±1.4% and 7.1±4.3% in Cat $K^{+/+}\rightarrow LDLR^{-/-}$ and Cat $K^{+/-}\rightarrow LDLR^{-/-}$ mice respectively, whereas a significant increase up to 11.9±3.8% was observed in Cat $K^{-/-}\rightarrow LDLR^{-/-}$ mice ($P<0.01$). Typical necrotic core areas are illustrated by arrows in Fig 4A. Cat $K^{-/-}\rightarrow LDLR^{-/-}$ mice also featured a significantly reduced frequency of elastic lamina fragmentation, 9 breakdowns in 13 mice, compared with 23 breakdowns in 13 mice and 16 breakdowns in 11 mice for Cat $K^{+/+}\rightarrow LDLR^{-/-}$ and Cat $K^{+/-}\rightarrow LDLR^{-/-}$ mice, respectively. Fragmentation of elastic lamina is indicated by arrows in Fig 4D. TUNEL staining also demonstrated that the amount of apoptotic cell death was significantly increased up to 3.0±0.8% ($P<0.01$) in Cat $K^{-/-}\rightarrow LDLR^{-/-}$ mice, as compared to 1.8±0.6% and 1.7±0.6% in Cat $K^{+/+}\rightarrow LDLR^{-/-}$ and Cat $K^{+/-}\rightarrow LDLR^{-/-}$ mice respectively (Fig 4E). A summary of the atherosclerotic lesion phenotypic changes is shown in figure 5.

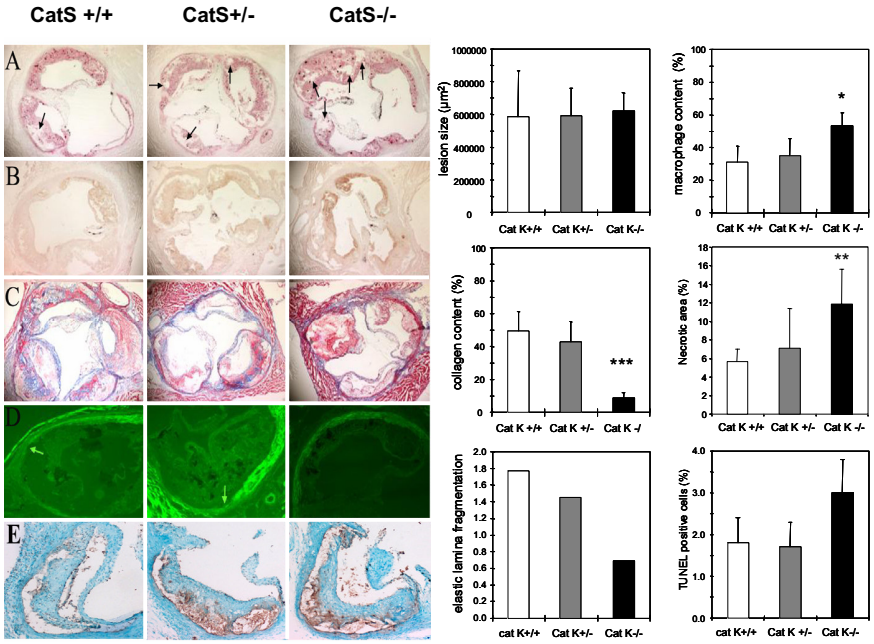

Figure 4. Disruption of leukocyte Cat K results in phenotypic changes in atherosclerotic lesions. Representative photos for (A) Lesion development. Typical necrotic area was indicated by arrows. (B) Rabbit-anti-mouse CD68 staining for mac

rophage. (C) Collagen content as visualized with aniline blue by Masson's Trichrome staining. (D) Fragmentation of elastic laminae (designated by arrows), which exhibit auto-fluorescence under a 465-495 nm excitation filter and a 515-555 nm emission filter. (E) TUNEL staining for apoptosis in atherosclerotic lesions.

Figure 5. Quantification of phenotypic changes in atherosclerotic lesions. The effect of leukocyte Cat K on atherosclerotic lesion size, macrophage content, collagen content, necrotic area, elastic lamina fragmentation and TUNEL positive nuclei was analyzed after 16 weeks Western-type diet feeding. Values represent the mean ± SEM of 13 mice for Cat $K^{+/+}$→ $LDLR^{-/-}$, 11 mice for Cat $K^{+/-}$→ $LDLR^{-/-}$ and 13 mice for Cat $K^{-/-}$→ $LDLR^{-/-}$ group. Statistically significant difference of *** stands for P< 0.001; ** for P< 0.01, and * for P<0.05, compared with Cat $K^{+/+}$→ $LDLR^{-/-}$ mice.

Potential Role of Cat K in the Apoptosis/Necrosis of Macrophages

The increased in situ cell death via necrosis and apoptosis in Cat $K^{-/-} \rightarrow LDLR^{-/-}$ mice prompted additional *in vitro* experiments to study the potential role of Cat K in macrophage cell death. We set up an *in vitro* assay to measure both CatK activity and cell death in oxLDL treated THP-1 cells and in the absence or presence of a specific Cat K inhibitor. This mimics the dynamic process of macrophage infiltration, oxLDL accumulation and subsequent cell death during atherogenesis. Treatment of THP-1 cells with oxLDL (24h, 100 µg/mL) induced a vivid red fluorescence indicating Cat K activity (Fig 6A). In the absence of Cat K inhibitor (vehicle alone), oxLDL treatment is accompanied by induction of apoptosis in 13.4±1.4% of the cells and necrosis in 25.9±1.4% of the cells (Fig 6C). Surprisingly, treatment of the cells in the presence of 1 µM of Cat K inhibitor augmented oxLDL-induced cell death such that 26.9±1.1% of the cells underwent apoptosis and 42.1±2.9% of the cells underwent necrosis (Fig 6D). Control experiments showed that treatment of THP-1 cells with 1 µM of Cat K inhibitor or vehicle alone (0.001% DMSO) had no effect on cell viability. Furthermore, treatment of the cells with inhibitor almost totally quenched Cat K activity demonstrating the effectiveness of the inhibitor (Fig 6B).

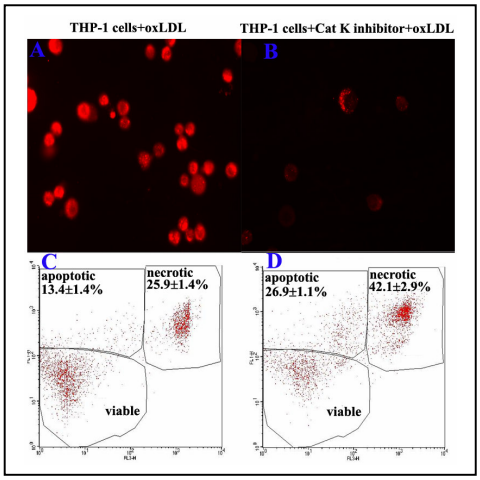

Figure 6. Potential role of Cat K in oxLDL-induced cell death in THP-1 Cells. **(A)** THP-1 cells, treated with oxLDL to induce cell death, were stained using a fluorogenic substrate for CatK (magic red Cat K kit), indicating the involvement of Cat K activity. **(B)** Diminished Cat K activity among THP-1 cells treated with oxLDL to induce cell death, upon the pre-treatment of cathepsin inhibitor, indicating the specificity of Cat K inhibitor. **(C)** oxLDL induced 13.4±1.39% and 25.94±1.44% of the THP-1 cells underwent apoptosis and necrosis respectively after 24 hours, as judged by the viable, apoptotic and necrotic populations by FACS. **(D)** Blocking Cat K activity by inhibitor increased the cell death up to 26.93±1.11% via apoptosis and 42.14±2.92% via necrosis in THP-1 cells. Values are mean ± SD of 4 samples, P< 0.01.

Discussion

Although Cat K attracted extensive attention with respect to its role in bone remodeling, its function in atherosclerosis has not yet been established since Sukhova *et al*[13] described that Cat K is abundantly expressed in macrophages and smooth muscle cells in human atheroma, suggesting a potential role in matrix remodeling. Previously, it has been shown that systemic disruption of Cat K resulted in impaired osteoclastic bone resorption[10;11]. Using a novel experimental approach (transplantation of Cat $K^{-/-}$ bone marrow progenitor cells into $LDLR^{-/-}$ mice), this study demonstrates, for the first time, the potential role of leukocyte Cat K in bone

remodeling. Absence of leukocyte Cat K, as expected, resulted in a significantly increased bone mineral density, which is consistent with previous findings. More important, the BMT approach possesses the advantage to specifically parse out the possible contributions of Cat K from hematopoietic origin vs. non-hematopoietic origin to both bone remodeling and atherogenesis. The most interesting and unexpected aspect of this study involves the effects of leukocyte Cat K silencing on atherogenesis. The absence of leukocyte Cat K in bone marrow progenitor cells did not affect plasma total cholesterol and triglyceride levels nor the atherosclerotic lesion size. However, the absence of leukocyte Cat K resulted in significant phenotypic changes of the lesions, with a dramatic decrease in collagen and a moderate increase in macrophage content.

Further characterization of the lesions revealed impaired elastic lamina fragmentation and an important increase of necrotic core area with leukocyte CatK deficiency. VSMCs, the major source of collagen in arteries, which migrate from the tunica media into the intima during late-stage atherosclerosis, require proteolytic degradation of elastin[25]. Due to the disruption of Cat K, the most potent mammalian elastase yet described[6], in freshly infiltrated monocytes during initial atherogenesis, this proteolytic degradation of elastin might be partially absent, which in turn hindered the entrance of SMCs crossing the internal elastic membrane into the intima. The well-preserved elastic lamina in absence of leukocyte Cat K thus might have resulted in the impaired migration of medial SMCs into the atherosclerotic lesions and thus impaired production of collagen. The greatly reduced amount of collagen was compensated by a modest increase in macrophage content and a considerable increase in necrotic core area. In fact, the observed increase in necrosis within the plaques of Cat $K^{-/-}\rightarrow LDLR^{-/-}$ mice might also have led to the enhanced release of all kinds of proteolytic enzymes, which might have contributed to the accelerated degradation of collagen.

In order to gain further insight into the effect of leukocyte Cat K deficiency on macrophage function, we performed *in vitro* experiments whereby Cat K activity was modulated by a recently established specific inhibitor[23]. OxLDL can induce cell death in macrophages/smooth muscle cells[26], endothelial[27] and lymphoid cells[28]. To further elucidate the mechanisms underlying the observed increase in necrotic core area in the absence of leukocyte CatK, we explored the potentially modulating effect of Cat K on oxLDL-induced cell death. In agreement with the data by Vicca *et al*[24] and Björkerud *et al*[26], we found oxLDL induced THP-1 cells to undergo both apoptosis and necrosis. Surprisingly, a selective Cat K inhibitor, which has no observed cytotoxicity at 1 μM, enhanced oxLDL-induced cell death of THP-1 cells almost 2-fold via both apoptosis and necrosis. This suggests that Cat K might have a beneficial effect on cell survival.

Taken together, we could envision the following sequence of events in atherogenesis: 1) monocytes infiltrate into the arterial wall and differentiate into macrophages; 2) these macrophages scavenge oxLDL and transdifferentiate into foam cells, meanwhile producing inflammatory cytokines and chemokines that attract more monocytes; 3) ongoing monocyte infiltration and accumulation ultimately results in apoptosis/necrosis due to the excessive production and uptake of oxLDL. Macrophage cell death via necrosis and defective clearance of apoptotic bodies results in the disruption of cell membrane/organelles and release of numerous inflammatory molecules, which eventually attract more monocytes into the arterial intima. In absence of leukocyte Cat K, the normal balance during atherogenesis between monocyte infiltration/foam cell accumulation vs. cell death appears to be disrupted, favoring augmented cell death via both apoptosis and

necrosis. Indeed, we do observe a significant increase in necrosis/apoptosis in the atherosclerotic lesions and a modest increase in macrophage content in the Cat $K^{-/-}$ → $LDLR^{-/-}$ mice. This increase in the amount of macrophages and necrosis/apoptosis should thus be considered as the final outcome, at a certain time point (16 weeks after BMT), of macrophage infiltration vs. an accelerated rate of cell death via both apoptosis and necrosis due to absence of Cat K.

Genetic manipulation of hematopoietic stem cells holds a great promise to treat human disease in the near future. It is thus interesting to investigate the function of genes from hematopoietic origin. The present study shows a well-defined role of leukocyte Cat K in the remodeling of both atherosclerotic lesion phenotype and bone resorption vs. formation. Pharmaceutical intervention of leukocyte Cat K might be an attractive strategy to treat osteoporosis. However, disruption of leukocyte Cat K unexpectedly resulted in more vulnerable atherosclerotic lesions (increased cell death via necrosis/apoptosis and decreased collagen). This observation establishes an important role of leukocyte Cat K in determining plaque composition and morphology, making it pathologically relevant to study the effect of therapeutically increased expression of Cat K on atherosclerotic lesion composition and plaque stability.

References

1. Li YP, Alexander M, Wucherpfennig AL, Yelick P, Chen W, Stashenko P. Cloning and complete coding sequence of a novel human cathepsin expressed in giant cells of osteoclastomas. *J Bone Miner Res*. 1995;10:1197-1202.
2. Rantakokko J, Aro HT, Savontaus M, Vuorio E. Mouse cathepsin K: cDNA cloning and predominant expression of the gene in osteoclasts, and in some hypertrophying chondrocytes during mouse development. *FEBS Lett*. 1996;393:307-313.
3. Shi GP, Chapman HA, Bhairi SM, DeLeeuw C, Reddy VY, Weiss SJ. Molecular cloning of human cathepsin O, a novel endoproteinase and homologue of rabbit OC2. *FEBS Lett*. 1995;357:129-134.
4. Tezuka K, Tezuka Y, Maejima A, Sato T, Nemoto K, Kamioka H, Hakeda Y, Kumegawa M. Molecular cloning of a possible cysteine proteinase predominantly expressed in osteoclasts. *J Biol Chem*. 1994;269:1106-1109.
5. Drake FH, Dodds RA, James IE, Connor JR, Debouck C, Richardson S, Lee-Rykaczewski E, Coleman L, Rieman D, Barthlow R, Hastings G, Gowen M. Cathepsin K, but not cathepsins B, L, or S, is abundantly expressed in human osteoclasts. *J Biol Chem*. 1996;271:12511-12516.
6. Bossard MJ, Tomaszek TA, Thompson SK, Amegadzie BY, Hanning CR, Jones C, Kurdyla JT, McNulty DE, Drake FH, Gowen M, Levy MA. Proteolytic activity of human osteoclast cathepsin K. Expression, purification, activation, and substrate identification. *J Biol Chem*. 1996;271:12517-12524.
7. Garnero P, Borel O, Byrjalsen I, Ferreras M, Drake FH, McQueney MS, Foged NT, Delmas PD, Delaisse JM. The collagenolytic activity of cathepsin K is unique among mammalian proteinases. *J Biol Chem*. 1998;273:32347-32352.
8. Gelb BD, Shi GP, Chapman HA, Desnick RJ. Pycnodysostosis, a lysosomal disease caused by cathepsin K deficiency. *Science*. 1996;273:1236-1238.
9. Johnson MR, Polymeropoulos MH, Vos HL, Ortiz de Luna RI, Francomano CA. A nonsense mutation in the cathepsin K gene observed in a family with pycnodysostosis. *Genome Res*. 1996;6:1050-1055.
10. Gowen M, Lazner F, Dodds R, Kapadia R, Feild J, Tavaria M, Bertoncello I, Drake F, Zavarselk S, Tellis I, Hertzog P, Debouck C, Kola I. Cathepsin K knockout mice develop osteopetrosis due to a deficit in matrix degradation but not demineralization. *J Bone Miner Res*. 1999;14:1654-1663.
11. Saftig P, Hunziker E, Wehmeyer O, Jones S, Boyde A, Rommerskirch W, Moritz JD, Schu P, von Figura K. Impaired osteoclastic bone resorption leads to osteopetrosis in cathepsin-K-deficient mice. *Proc Natl Acad Sci U S A*. 1998;95:13453-13458.
12. Votta BJ, Levy MA, Badger A, Bradbeer J, Dodds RA, James IE, Thompson S, Bossard MJ, Carr T, Connor JR, Tomaszek TA, Szewczuk L, Drake FH, Veber DF, Gowen M. Peptide aldehyde inhibitors of cathepsin K inhibit bone resorption both in vitro and in vivo. *J Bone Miner Res*. 1997;12:1396-1406.
13. Sukhova GK, Shi GP, Simon DI, Chapman HA, Libby P. Expression of the elastolytic cathepsins S and K in human atheroma and regulation of their production in smooth muscle cells. *J Clin Invest*. 1998;102:576-583.
14. Linton MF, Atkinson JB, Fazio S. Prevention of atherosclerosis in apolipoprotein E-deficient mice by bone marrow transplantation. *Science*. 1995;267:1034-1037.

15. Van Eck M, Herijgers N, Yates J, Pearce NJ, Hoogerbrugge PM, Groot PH, Van Berkel TJ. Bone marrow transplantation in apolipoprotein E-deficient mice. Effect of ApoE gene dosage on serum lipid concentrations, (beta)VLDL catabolism, and atherosclerosis. *Arterioscler Thromb Vasc Biol*. 1997;17:3117-3126.
16. Ishibashi S, Brown MS, Goldstein JL, Gerard RD, Hammer RE, Herz J. Hypercholesterolemia in low density lipoprotein receptor knockout mice and its reversal by adenovirus-mediated gene delivery. *J Clin Invest*. 1993;92:883-893.
17. Ishibashi S, Goldstein JL, Brown MS, Herz J, Burns DK. Massive xanthomatosis and atherosclerosis in cholesterol-fed low density lipoprotein receptor-negative mice. *J Clin Invest*. 1994;93:1885-1893.
18. Guo J, Van Eck M, Twisk J, Maeda N, Benson GM, Groot PH, Van Berkel TJ. Transplantation of monocyte CC-chemokine receptor 2-deficient bone marrow into ApoE3-Leiden mice inhibits atherogenesis. *Arterioscler Thromb Vasc Biol*. 2003;23:447-453.
19. Groot PH, van Vlijmen BJ, Benson GM, Hofker MH, Schiffelers R, Vidgeon-Hart M, Havekes LM. Quantitative assessment of aortic atherosclerosis in APOE*3 Leiden transgenic mice and its relationship to serum cholesterol exposure. *Arterioscler Thromb Vasc Biol*. 1996;16:926-933.
20. Virmani R, Kolodgie FD, Burke AP, Farb A, Schwartz SM. Lessons from sudden coronary death: a comprehensive morphological classification scheme for atherosclerotic lesions. *Arterioscler Thromb Vasc Biol*. 2000;20:1262-1275.
21. Gavrieli Y, Sherman Y, Ben Sasson SA. Identification of programmed cell death in situ via specific labeling of nuclear DNA fragmentation. *J Cell Biol*. 1992;119:493-501.
22. Van Berkel TJ, De Rijke YB, Kruijt JK. Different fate in vivo of oxidatively modified low density lipoprotein and acetylated low density lipoprotein in rats. Recognition by various scavenger receptors on Kupffer and endothelial liver cells. *J Biol Chem*. 1991;266:2282-2289.
23. Wang D, Pechar M, Li W, Kopeckova P, Bromme D, Kopecek J. Inhibition of cathepsin K with lysosomotropic macromolecular inhibitors. *Biochemistry*. 2002;41:8849-8859.
24. Vicca S, Hennequin C, Nguyen-Khoa T, Massy ZA, Descamps-Latscha B, Drueke TB, Lacour B. Caspase-dependent apoptosis in THP-1 cells exposed to oxidized low-density lipoproteins. *Biochem Biophys Res Commun*. 2000;273:948-954.
25. Sukhova GK, Zhang Y, Pan JH, Wada Y, Yamamoto T, Naito M, Kodama T, Tsimikas S, Witztum JL, Lu ML, Sakara Y, Chin MT, Libby P, Shi GP. Deficiency of cathepsin S reduces atherosclerosis in LDL receptor-deficient mice. *J Clin Invest*. 2003;111:897-906.
26. Bjorkerud B, Bjorkerud S. Contrary effects of lightly and strongly oxidized LDL with potent promotion of growth versus apoptosis on arterial smooth muscle cells, macrophages, and fibroblasts. *Arterioscler Thromb Vasc Biol*. 1996;16:416-424.
27. Harada-Shiba M, Kinoshita M, Kamido H, Shimokado K. Oxidized low density lipoprotein induces apoptosis in cultured human umbilical vein endothelial cells by common and unique mechanisms. *J Biol Chem*. 1998;273:9681-9687.
28. Escargueil-Blanc I, Salvayre R, Negre-Salvayre A. Necrosis and apoptosis induced by oxidized low density lipoproteins occur through two calcium-dependent pathways in lymphoblastoid cells. *FASEB J*. 1994;8:1075-1080.